19. Davidson, E. A., Verchot, L. V., Cattanio, J. H., Acjerman, I. L. and Carvalho, J. E. M., Effects of soil water content on soil respiration in forests and cattle pastures of eastern Amazonia. *Biogeochemistry*, 2000, **48**, 53–69.
20. Sotta, E. D., Meir, M., Malhi, Y., Nobre, A. D., Hodnett, M. and Grace, J., Spatial heterogeneity of soil respiration and related properties at the plant scale. *Global Change Biol.*, 2004, **10**, 601–617.
21. Malhi, Y. and Grace, J., Tropical forests and atmospheric carbon dioxide. *Trees*, 2000, **15**, 332–337.
22. Luo, Y., Wan, S., Hui, D. and Wallace, L. L., Acclimatization of soil respiration to warming in a tall grass prairie. *Nature*, 2001, **413**, 662–625.
23. Zhou, L. X., Yi, W. M., Yi, Z. G. and Ding, M. M., Soil microbial characteristics of several vegetations at different elevation in Dinghushan Biosphere Reserve. *Trop. Subtrop. For. Ecosyst. Res.*, 2002, **9**, 169–174.
24. Kaye, J. P. and Hart, S. C., Restoration and canopy type effects on soil respiration in a ponderosa pine – Bunchgrass ecosystem. *Soil Sci. Soc. Am. J.*, 1998, **62**, 1062–1072.
25. Holt, J. A., Hodgen, M. J. and Lamb, D., Soil respiration in the seasonally dry topics near Townville, North Queensland. *Aust. J. Soil Res.*, 1990, **28**, 737–745.
26. Birch, H. F., The effect of soil drying on humus decomposition and nitrogen availability. *Plant Soil*, 1958, **10**, 9–31.
27. Lopez, B., Sabate, S. and Gracia, C., Fine roots dynamics in a Mediterranean forest: Effects of drought and stem density. *Tree Physiol.*, 1998, **18**, 601–606.
28. Tang, X. L., Zhou, G. Y., Liu, S. G., Zhang, D. Q., Liu, S. Z., Li, J. and Zhou, C. Y., Dependence of soil respiration on soil temperature and soil moisture in successional forests in Southern China. *J. Integrat. Plant Biol.*, 2006, **48**, 654–663.
29. Joffre, R., Ourcival, J. M., Rambal, S. and Rocheteau, A., The key role of top soil moisture on CO_2 efflux from a Mediterranean *Quercus ilex* forest. *Ann. For. Sci.*, 2003, **60**, 519–526.
30. Adachi, M., Bekku, Y. S., Rashidah, W., Okuda, T. and Koizumi, H., Differences in soil respiration between different tropical ecosystems. *Appl. Soil Ecol.*, 2006, **34**, 258–265.
31. Singh, J. S., Raghubanshi, A. S., Singh, R. S. and Srivastava, C., Microbial biomass acts as a source of plant nutrients in dry tropical forest and savanna. *Nature*, 1989, **338**, 499–500.
32. Singh, J. S. and Gupta, S. R., Plant decomposition and soil respiration in terrestrial ecosystems. *Bot. Rev.*, 1977, **43**, 449–529.

ACKNOWLEDGEMENTS. We thank the Department of Biotechnology, New Delhi, for financial support. We also thank Prof. P. Gunasekaran, UGC Centre for Excellence in Genomic Sciences, Madurai Kamaraj University, Madurai for providing Licor 6400-09 soil CO_2 flux chamber and the anonymous referees for their valuable comments.

Received 14 December 2007; revised accepted 14 May 2008

Influences of look angle and look direction of space-borne SAR sensor in geological feature delineation in Metasedimentary terrain of Kurnool Group of rocks, Andhra Pradesh

Arindam Guha*, K. Vinod Kumar and M. V. V. Kamaraju

Geosciences Division, National Remote Sensing Agency, Balanagar, Hyderabad 500 625, India

The role of look angle and look direction of space-borne SAR sensors in enhancing signatures of geological elements is an important aspect of study. In the present study, two different look angle (IS2 and IS4) data of ENVISAT ASAR are compared to evaluate the significance of look angle in enhancing different lithovariants and structures of the Proterozoic metasedimentary terrain. The ascending and descending modes of data acquisition of ENVISAT ASAR also help to study the significance of look direction in enhancing or subduing geological features. Geometric distortion is similar in both look angles. Low-dipping sedimentary terrain with steep mesa, butte and cuesta ridges creates layover on images of IS2 (18°–25°) and IS4 (28°–36°) acquisition of ENVISAT, but low look angle facilitates less shadow zones at the back slope portion and helps in finding important geological structures. Alternate polarization channels of ENVISAT ASAR are useful in enhancing the lithovaraints based on polarization signatures characteristically developed over each rock type due to variation in surface roughness and moisture content of each rock type. Separabilty of one rock type from another based on polarization signatures is better in low look-angle data. Drainages on the other hand, are enhanced in high look-angle data as the specular surface of drainage returns appreciable energy in low look-angle acquisition. In the present study it is found that lineaments of variable trends can be mapped better from dual look-direction data.

Keywords: Image fusion, litho unit, look angle, look direction, sedimentary terrain.

IMAGING radars are operated in the microwave range of the electromagnetic spectrum[1] at wavelengths from about 1 cm to 1 m. SAR provides valuable information on surface roughness, soil moisture, topography and drainage pattern of a terrain[2]. SAR also has limited capabilities to penetrate through the soil cover and thereby can provide valuable information about *in situ* rock type and subsurface structure. Moreover, SAR techniques have the efficiency to provide relatively coarser resolution where minor details and variations are suppressed. Owing to this

*For correspondence. (e-mail: arindam_iit@rediffmail.com)

fact, SAR images are helpful in regional landform studies, especially if the variations in landform units are manifested in terms of differences in surface roughness, relief, moisture, etc. Lineaments are well manifested in radar image and give information about the strikes or trends of geological structures like faults, joints, shear planes, fractures, bedding, gneissosity planes, etc. It must be emphasized that often some of the geological features, especially linear structures are better observed on SAR images than the corresponding VNIR or photographic images[1]. A brief account of microwave remote sensing in geological applications is discussed by Singhroy *et al.*[3]. They have reviewed the role of SAR look angle in enhancing terrain features in low relief environment. It has been observed that small to intermediate incident angle (10°–25°) is suitable since it produces maximum relief enhancement, but larger incident angle will also result in acceptable terrain rendition, by increasing the terrain textural contrasts[4]. But most of the backscatter contrasts observable in space-borne radar images are easier to detect at lower look angle[1].

Geological structures give topographic impressions in varied direction according to the trend of the structures. The capability of synthetic aperture radar to view from different look directions enhances topographical/geomorphological signatures characteristic to a specific structure. High-angle faults and joint planes give a linear impression (linearly arranged vegetation, linear scrap face, etc.) on low-dipping/horizontal formation, which can be picked up well in the SAR data. Linear structures have various trends and SAR look direction plays an important role in enhancing or subduing linear structures. Some structures get subdued in a particular look-direction data, while they appear better in another look-direction data.

The main focus of the present work is to identify the utilities of two look-angle C-band ENVISAT ASAR data with HH, HV polarization in both ascending and descending modes of acquisition for geological studies. The main thrust remains in understanding the effects of look angle and look direction of SAR images in geological structure delineation and sedimentary lithounit demarcation.

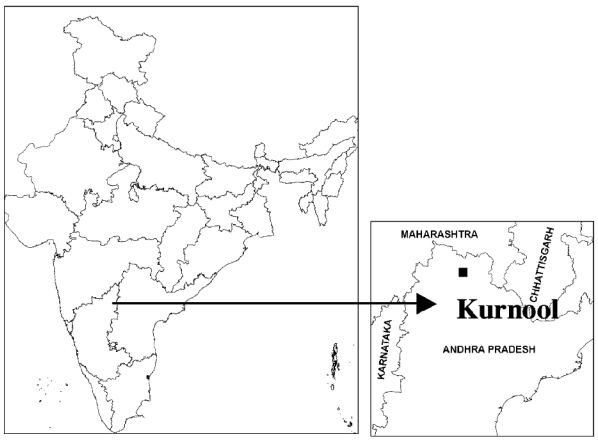

Figure 1. Location map of study area.

The study area is located SW of Kurnool, Andhra Pradesh. The area falls within the north latitudes 15°05′00″ to 15°18′00″ and east longitudes 77°55′00″ to 78°16′00″, and covers parts of Survey of India toposheet nos 57I/3 and 57I/4. The study area is well connected to Hyderabad, the state capital, by the state and national highways (Figure 1).

The present study area is mainly represented by sedimentary rocks of the Kurnool Group, which overlies the Cuddapahs Supergroup of rocks and is separated from Cuddapah by the presence of an unconformity. The Kurnool Supergroup of rocks is formed in two sub-basins, namely Kurnool and Palnad; the present study encompasses only part of the Kurnool sub-basin. Generalized stratigraphy[5] and basic description of the rock units are given in Table 1.

The major rock units studied using microwave data belong to the Kurnool Group of rocks, which is upper Proterozoic in age. The Kurnool basin is a half-graben basin created by intracratonic fault. Cuddapah rocks are exposed in the central and western parts of the study area. Cuddapah rocks are deposited in the intracratonic basin and are separated from the Kurnool Group of rocks by an unconformity. Dharwar rocks occur in patches within the Peninsular Gneissic Complex (PGC). Dolerite dykes are also present within the Archaean rocks and are faulted.

The satellite ENVISAT was launched in March 2002, by the European Space Agency. Its largest single instrument is the Advanced Synthetic Aperture Radar (ASAR) operated at the C-band (5.331 GHz). In the alternating polarization mode, two images in two-polarization mode (HH & VV, HH & HV or VV & VH) can be acquired with ground resolution of 30 m, sampled at 12.5 m. C-band APP (alternate polarization) data (HH and HV polarization) acquired in two-beam mode (i.e. for two look angles) during September 2005 were used for the present work for two beams (IS2 and IS4). Both ascending and descending pass data for each beam are used for the study. Geological map prepared by the Geological Survey of India has also been used as reference data. The specifications of SAR data used for the present study are given Table 2.

ENVISAT ASAR datasets were retrieved from the original raw data format to a software-compatible format, with the help of available image processing software (ENVI 4.2 and ERDAS imagine 8.6). Each image datum has two channels, each related to polarization return of backscatter signal. In the present datasets, alternate polarization (HH & HV) channels are used. These datasets contain two look-angle data in IS2 (18°–26°) and IS4 (30°–36°). Each look-angle datum contains two data subsets, one each for the ascending and descending modes of acquisition. Therefore, four separate datasets were proc-

Table 1. Generalized stratigraphy and basic description of the rock units

Supergroup	Group	Formation	Lithology
	Kurnool Group	Nandyal Shale	Purple-coloured ferruginous shale
		Koilkuntla Limestone	Argillaceous limestone
		Paniam Quartzite	Quartz arenite with pinnacle structure
		Owk Shale	Ochrous shale
		Narji Limestone	Flaggy limestone
		Banganapally Quartzite	Conglomerate, quartzite
		Unconformity	
Cuddapah Supergroup	Nallamalai Group	Quartzite, Shale, shale with phyllite and dolomite	
		Angular unconformity	
	Chitravati Group	Conglomerate, quartzite, shale, tuff, dolomite	
		Disconformity	
	Papaghni Group	Dolomite, chert/mudstone, quartzite, conglomerate and basic sills/tuffs	
		Unconformity	
Archaean	Dharwar Supergroup	Metabasalt, amphibolite, metadacite, etc.	
	Peninsular Gneissic Complex	Granite gneiss, hornblende biotite gneiss, K-rich grainte	

Table 2. Specifications of SAR data used in the present study

Data	Look angle	Polarization	Look direction	Swath (km)	Ground resolution (m)	Acquisition date	Bands (cm)
ENVISAT ASAR data	IS2 (18°–26°)	HH	East (ascending)	100	30	September 2005	C-band (5.8 cm)
		HV	West (descending)	100	30	September 2005	C-band (5.8 cm)
	IS4 (30°–36°)	HH	East (ascending)	100	30	September 2005	C-band (5.8 cm)
		HV	West (descending)	100	30	September 2005	C-band (5.8 cm)

essed for the present study. Each datum was co-registered and for better interpretability and to enhance the contrast between features in ENVISAT ASAR data, the Lee-Sigma filter was used to reduce speckles from the image. In the speckle suppression procedure, a 3×3 window with single iteration was found sufficient to enhance the contrast between image features for further analysis. The Lee-Sigma filter shows good edge-preserving capability and is an effective speckle-removal filter[6]. In an effort to study the absolute scattering amount of each litho-variant and compare the variability of scattered microwave energy of rocks, the scattering coefficient σ° was calculated[7]. The value of σ° depends on the physical and electrical properties of the reflecting material, and on the wavelength, polarization and illumination angle of incidence. σ° was calculated by creating A model in THE ERDAS imagine 9.1 software. The basic equation used for THE calculation of σ° is as follows:

$$\sigma^\circ = 10*\log_{10}[(DN)^2/K)*\sin(I)], \quad (1)$$

where I is the average incident angle for a particular beam, K a constant retrieved from the source image header information file and DN the digital number of the source image.

σ° can be computed for ENVISAT ASAR data using eq. (1). In the absence of the incident angle map for the area, the mean value of look angle for each beam was taken as the incident angle of the area. This assumption is also based on the fact that the terrain is almost horizontal and therefore, slope has less contribution to backscattering coefficient. This holds good for flat-topped mesa and flat-valley areas, but not in the ridge slope area. This assumption would not be applicable across the swath. Therefore, the training areas for comparing backscattering coefficients of different rocks should fall close to each other, so that variability of scattering coefficient due to swath can be reduced. Therefore, whenever the backscattering coefficient is studied for rocks in the present study, samples are identified in either flat-topped mesa area or flat-valley area, and samples are close to each other with reference to beam width of the sensor.

Data processing of SAR images in the present study can be broadly subdivided into two major domains: composite image preparation and comparative analysis of back-scattering coefficients of different rock types for different look angles. Field work was carried out during December 2006, to evaluate the geological and geomorphological information of the study area already extracted from the ENVISAT ASAR data. The fieldwork was also aimed to identify some unweathered/less weathered rock exposures. These exposures are identified in images and backscattering coefficients are calculated for these exposures to characterize and discriminate rocks on the basis of scattering coefficient.

In the present study, ENVISAT ASAR data with look-angle data and alternate polarization as well as both look

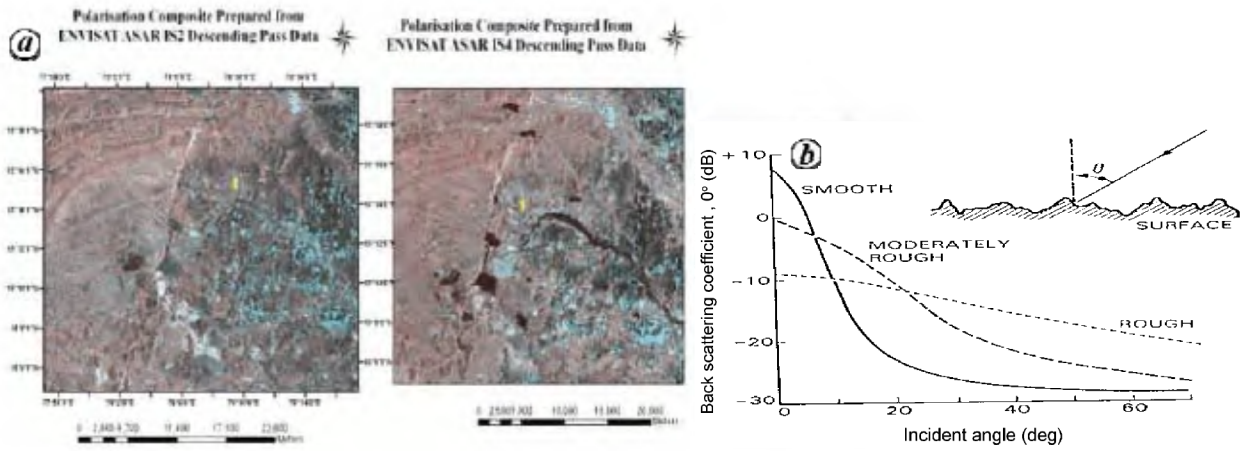

Figure 2. ***a***, Water bodies and drainages (marked by 1) can be better mapped in high look-angle data. In FCC (false colour composite), polarization of channel is displayed in RGB colour space R = HV, G = HH and B = HH. ***b***, Typical radar backscatter curves for smooth, moderately rough and very rough surfaces. As the incident angle decreases, the probability of greater backscatter increases, especially as the target becomes smooth.

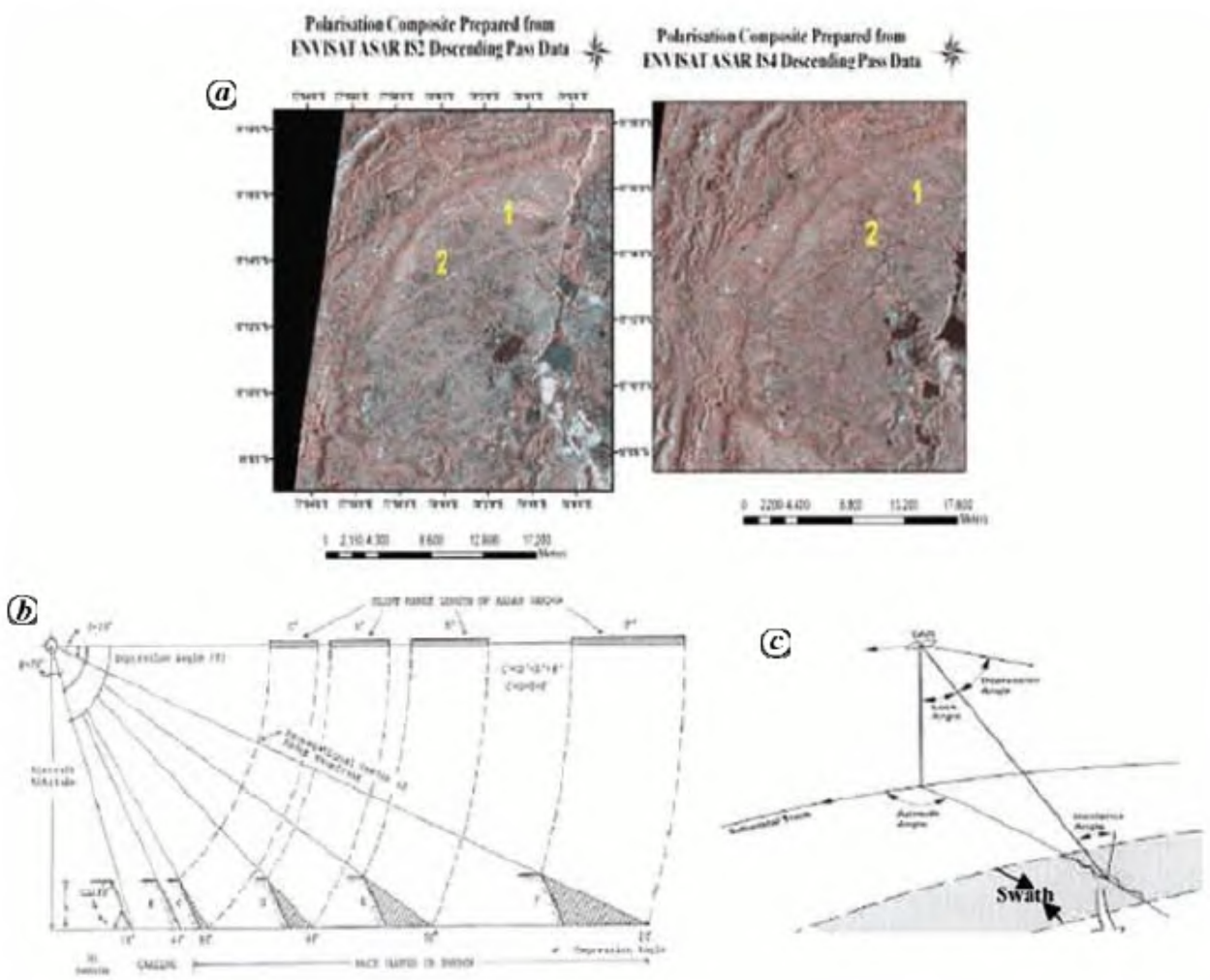

Figure 3. ***a***, Geological structures are often better delinetaed in low-angle data as high look-angle acquisition creates darker zones in the backslope portion of vertical steep slopes and therefore makes it difficult in delineating lineaments on the basis of geomorphic expression. ***b***, Relation between depression angle and shadow[9]. ***c***, Relation between look angle, depression angle and incident angle. The look angle and incident angle are the same for a small area, if the terrain is horizontal.

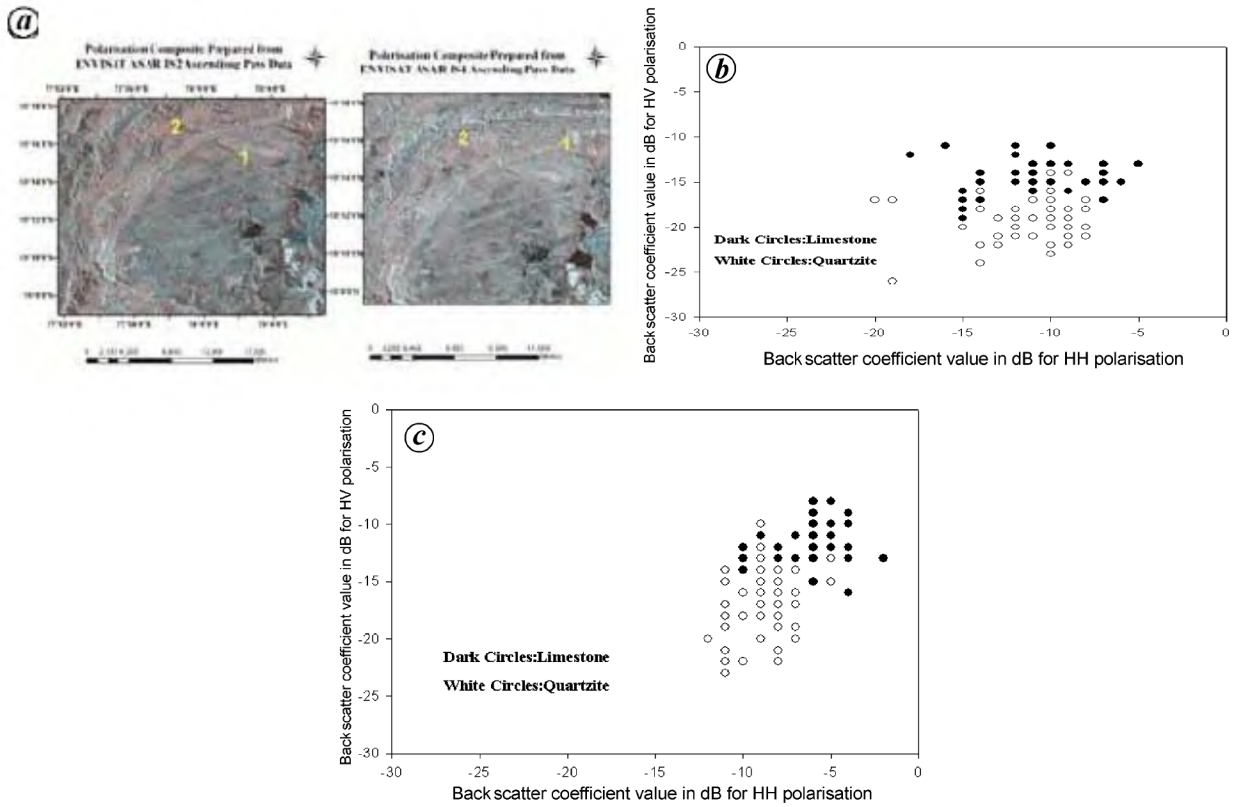

Figure 4. *a*, Quartzite (1) and shaly limestone (2) are better delineated in low look-angle data. *b*, *c*, Plot of backscattering coefficients in high (*b*) and low (*c*) look-angle data.

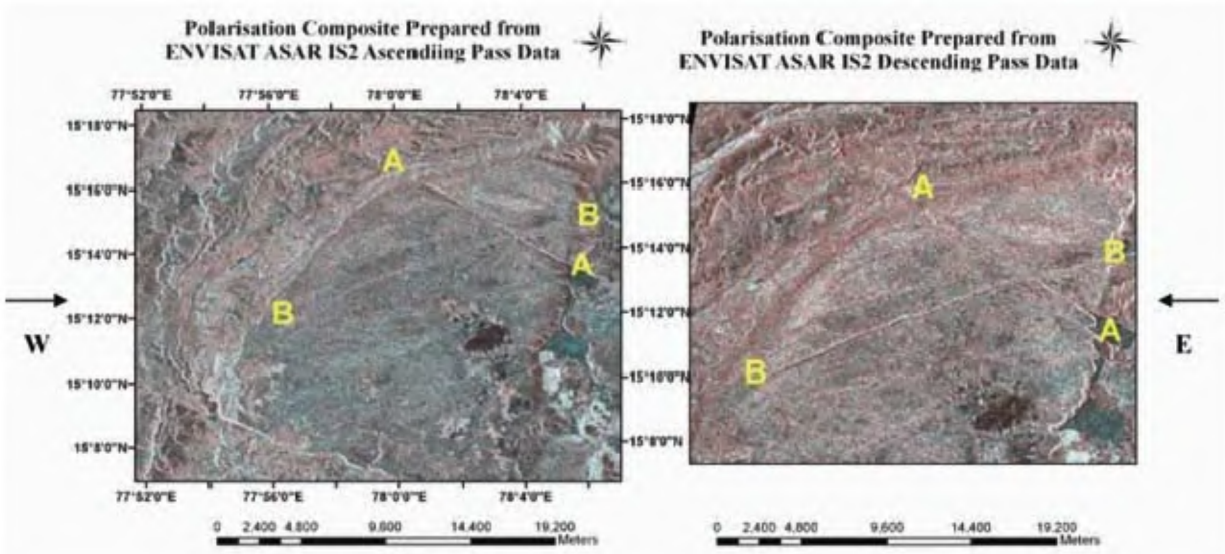

Figure 5. Lineaments perpendicular to look direction are conspicuous and those parallel to the look direction are subdued in different look-direction composites. In FCC, polarization of channel is displayed in RGB, R = HV, G = HH and B = HH. Arrow refers to look direction.

directions have been evaluated. Look angle plays an important role in delineating geological structures by enhancing tectonic geomorphological features and discriminating different lithologies in terms of surface roughness and surface dielectric constant. Figure 2 *a* illustrates how high look angle-data enhance drainages and water bodies com-

pared to low look-angle data. Figure 2 *b* demonstrates how specular features give higher responses in low look-angle data. As the look angle increases, the return from specular features get reduced and therefore, high look-angle data are useful in delineating drainages and water bodies, which appear dark in high look-angle data. Figure 3 *b* illustrates how shadows are generated in the back slope portion of high-angle sloping geomorphic units. These shadows will depreciate the quality of the image and suppress the geological details. However, the lineaments (1, 2) are enhanced in low look-angle data (Figure 3 *a*). Backscattering coefficient of a particular rock surface also changes with the change in look angle[8]. The study of backscattering coefficients of quartzite and limestone (Figure 4 *a*) shows that low look-angle data differentiate rock units better than high look-angle data. Plots of backscattering coefficients of quartzite and shaly limestone (Figure 4 *b* and *c*) show that low look-angle data enhance the contrast between two lithovariants of the sedimentary terrain on the basis of backscattering return. Also, HV polarization appears to differentiate quartzite and limestone better.

A geological lineament, trending NE–SW (B–B in Figure 5) gets subdued in the IS2 ascending pass image, while the same lineament is more enhanced in descending pass data. Reverse is the case for the lineament A–A. It has been observed that lineaments trending parallel to a particular look direction get subdued and those which are across or perpendicular to a look direction are enhanced. Therefore, it is necessary to study both the look directions to map the lineaments of different trends.

The study of space-borne SAR data for geological information synthesis reveals that look angle and look direction play an important role in the discrimination of lithounits and structural elements in metasedimentary terrain.

Look direction plays a major role in delineating structures. Lineaments of variable trend can be better mapped from dual look-directional data. Lineaments with trends parallel to the look direction get subdued, whereas those perpendicular to the look direction are enhanced.

Look angle should be chosen according to the terrain characteristics to reduce the radar geometrical distortions. Horizontal or low-dipping sedimentary terrain with mesa, butte and cuesta type of landform ridges (high slope angle) can be better mapped with low look-angle data. Drainages can be better studied in moderate to high look-angle data.

Separatibility of limestone and quartzite on the basis of backscattering coefficients is found better in lower look-angle data compared to higher look-angle data.

1. Ford, J. P. *et al.*, Radar geology, principles and application of imaging radar. In *Manual of Remote Sensing* (eds Henderson, F. M. and Anthony Lewis, A. J.), John Wiley, 1998, vol. 2, pp. 511–562.
2. Gupta, R. P., *Remote Sensing Geology*, Springer-Verlag, 2003, 2nd edn, pp. 317–392.
3. Singhroy, V. *et al.*, Radarsat and radar geology in Canada. *Can. J. Remote Sensing*, 1993, **19**, 338–349.
4. Singhroy, V. and Saint-Jean, R., Effects of relief on the selection of Radarsat-1 incident angle for geological applications. *Can. J. Remote Sensing*, 1999, **25**, 221–228.
5. Nagaraja Rao, B. K., Rajurkar, S. T., Ramalingaswamy, G. and Ravindra Babu, B., Stratigraphy, structure and evolution of Cuddapah basin. In *Purana Basins of Peninsular India*, Geological Society of India, Memoir, 1987, vol. 6, pp. 33–86.
6. Rivera Rio, J. N. and Lozano-Garcia, D. F., Spatial filtering of radar data (radarsat) for wetlands (brackish marsh) classification. *Remote Sensing Environ.*, 2000, **73**, 143–151.
7. Ulaby, F. T., Moore, R. K. and Fung, A. K., *Microwave Remote Sensing Active and Passive, From Theory to Application*, 1990, vol. 3 (reprint edition), pp. 1797–1848.
8. Singhroy, V. and Katrin, M., Geological case studies related to Radarsat-2. *Can. J. Remote Sensing*, 2004, **30**, 893–902.
9. Lewis, A. J., Geomorphic evaluation of radar imagery of Southwestern Panama and North-western Colombia, CRES Technical Report, University of Kansas, 1971, pp. 133–138.

ACKNOWLEDGEMENTS. We thank the Director, NRSA, Hyderabad for support and encouragement during the course of this work. We are grateful to Dr P. S. Roy for encouragement and Dr Shiv Mohan for valuable suggestions. We also thank the anonymous reviewer for his comments and suggestions that helped to improve the manuscript.

Received 1 August 2007; revised accepted 5 May 2008

Regional metamorphism in the Haimanta Group of rocks, Sutlej river valley, NW Himalaya, India

S. S. Thakur* and K. Tripathi

Wadia Institute of Himalayan Geology, 33 GMS Road, Dehra Dun 248 001, India

Pelitic rocks of the Haimanta Group exposed in the Sutlej river valley, NW Himalaya have undergone kyanite-grade regional metamorphism. The rocks show evidences of two phases of deformation (D_1 and D_2), which have led to the development of S_1 and S_2 schistosities respectively. Numerous granite veins fed by the lower Palaeozoic Kinnaur Kailash granite pluton have intruded the area parallel to the S_1 schistosity of the host rocks. Many of the granite veins are folded by D_2 deformation, and have intruded either before or during the early part of D_2 deformation. Pelitic schists in the area contain porphyroblasts of garnet, staurolite and kyanite. Elongated grains of kyanite and staurolite aligned parallel to S_1 schistosity show microfolding related to D_2 deformation, and are interpreted to have grown during the early part of D_2 deformation. Garnet porphyroblasts show reverse chemical zoning due to retrogression. Geothermobarometric calculations yield peak P–T conditions of 9.1 kbar and 625°C.

*For correspondence. (e-mail: satya_edu1974@yahoo.co.in)